Reverse time migration of multiples: Applications and challenges

Zhiping Yang[1], Jeshurun Hembd[1], Hui Chen[1], and Jing Yang[1]

Abstract

Marine seismic acquisitions record both primary and multiple wavefields. In a typical processing sequence, multiple energy is removed from the data before migration. However, valuable information might be contained in the multiple wavefield. A modification is proposed to the standard reverse time migration (RTM) algorithm to enable correct imaging between the primary wavefield and the first-order multiple wavefield. The advantages of this modification, reverse time migration of multiples (RTMM), are evaluated through three real data-processing projects and identified three key advantages. First, RTMM can recover small-angle reflections critical for shallow-water imaging that are missing in the primary wavefield. Second, RTMM has a wider illumination coverage, which significantly extends the image for an ocean-bottom node (OBN) project. Third, RTMM produces an image complementary to the primary image in a complex geologic setting, possibly assisting with interpretation. In addition, a synthetic study is presented of two types of cross-talk noise that hinder the full potential of RTMM, and corresponding practical strategies are proposed to handle them.

Introduction

A unique feature of marine seismic acquisitions is the existence of a flat and highly reflective water-air interface. For seismic energy, this interface acts as a mirror. The recorded signal contains both the primary and additional wavefields that could bounce back and forth between the subsurface reflectors and the flat water-air interface one or more times. A wavefield that has been reflected more than once by subsurface reflectors is known as a multiple wavefield. The coexistence of the multiple wavefield with the primary wavefield creates challenges as well as opportunities for seismic imaging.

The traditional approach is to consider the multiple wavefield noise and to remove it from the primary wavefield. However, the multiple wavefield is not just noise. Instead, valuable hidden information can be discovered with the proper migration algorithms (Berkhout and Verschuur, 2011; Lu et al., 2011).

Reverse time migration is accepted widely as the standard wave-equation migration algorithm. It forward-propagates a synthetic impulse to simulate the source wavefield and backward-propagates the primary wavefield to reconstruct the receiver wavefield. After both wavefields are fully propagated, an imaging condition is applied to create the seismic image. To use the multiple wavefield, we can replace the impulse with the recorded primary wavefield for the source wavefield and with the first-order multiple wavefield for the receiver wavefield. With a similar imaging condition, we can form a seismic image as well. We named this approach reverse time migration of multiples (RTMM) (Yang et al., 2013). With these choices for the source and receiver wavefields, RTMM can form a proper image using the illumination power hidden in the first-order free-surface multiples.

There are three major advantages of RTMM compared with the standard, primary-only RTM. First, RTMM allows more small-angle reflections to be used for imaging. This enables more accurate imaging of shallow reflectors (in particular, the water bottom), which improves the modeling of multiples in shallow-water data sets. Second, RTMM provides wider illumination coverage. This helps to extend the seismic image of the ocean-bottom node data considerably in a combined OBN and wide-azimuth towed-streamer (WATS) model-building and imaging project. Third, RTMM has a denser and more balanced illumination, which enables it to produce an image complementary to the primary image in complex geologic settings where the primary illumination is less than optimal.

RTMM for shallow imaging

In shallow-water surveys, water-layer multiple removal can be challenging. The typical demultiple technique for deepwater surveys is surface-related multiple elimination (SRME). However, good results depend on adequate sampling of all primary reflections, including near-angle reflections at the water bottom. These water-bottom reflections often are missing from shallow-water data sets because of the lack of near-offset data. In this case, a model-based water-layer demultiple (MWD) process is a better option for attenuating water-bottom-related multiples (Wang et al., 2011).

The prerequisite for a successful MWD is an accurate water-bottom horizon, usually interpreted on a migrated volume. However, the water bottom often is imaged poorly by algorithms that image primaries only because of the lack of small-angle reflections. Figure 1 shows an example of waterflood images in the crossline view for a shallow-water imaging project in the Gulf of Mexico. The sail-line spacing for this acquisition was 600 m. The acquisition footprint is apparent in the crossline view of the standard RTM

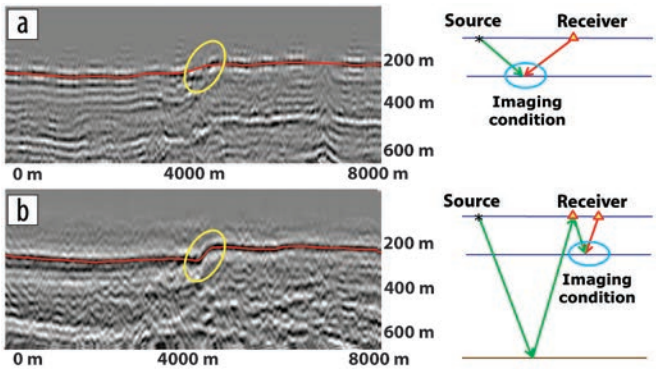

Figure 1. Waterflood images (crossline view) of (a) standard RTM and (b) RTMM, along with their corresponding schematic raypath diagrams. Courtesy of CGG. Used by permission.

[1]CGG.

http://dx.doi.org/10.1190/tle34070780.1.

image. In comparison, the RTMM image shows a focused and continuous water bottom.

This dramatic difference is explained by the schematic raypath diagram next to the corresponding images. For primary imaging, the minimum reflection angle quickly approaches the critical angle as the receivers extend in the crossline direction. This poor sampling in reflection angle introduces character changes into the migrated wavelet in the seismic image, which appear as alternating patterns of strong and weak amplitudes. For RTMM, the illumination of the water bottom is no longer the impulse at the shot location. Instead, all the received primary energy serves as the illumination source. The reflections from a deeper subsurface structure can generate a much smaller angle of reflection at the water bottom to be imaged by RTMM. The abundant small-angle reflections of RTMM also help to define details about the water-bottom horizon (yellow circle in Figure 1) that otherwise would be missed completely by standard RTM. The red curves overlaid on the two images are the water-bottom horizons obtained by autotracking using the same parameters.

Figure 2 shows the water-bottom horizons generated from the two waterflood images in Figure 1. The water-bottom horizon from the standard RTM (Figure 2a) shows horizontal stripes, i.e., the acquisition footprint. By comparison, the water-bottom horizon from RTMM (Figure 2b) is nearly artifact free, with high-resolution detail of the water-bottom topography.

The accurate water-bottom horizon generated from the RTMM image results in a more precise multiple model and a cleaner data set after demultiple. Figure 31 and 3b shows the MWD multiple models based on horizons from the standard RTM image and the RTMM image, respectively. Figures 3d and 3d show the corresponding demultiple outputs. The residual multiple is less obvious in Figure 3d (using the more precise water-bottom horizon from RTMM) than in Figure 3c (using the water-bottom horizon from standard RTM).

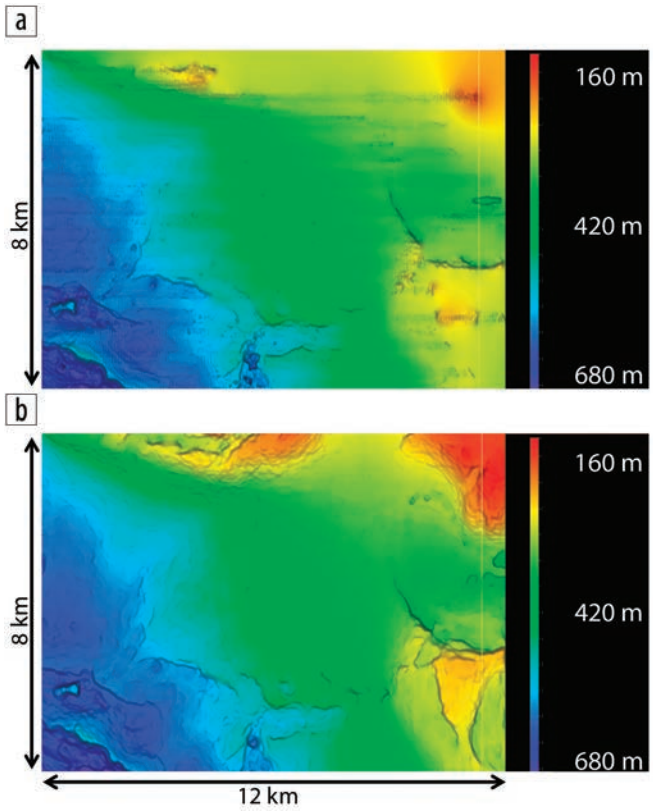

Figure 2. Water-bottom horizon generated from the (a) standard RTM image and (b) RTMM image. Color represents depth. Courtesy of CGG. Used by permission.

RTMM for OBN

Ocean-bottom node acquisitions have gained popularity because of their higher signal-to-noise ratio (S/N), full-azimuth coverage, and complete offset coverage from near to far. However, the operational cost of an OBN acquisition is still significantly higher than that of a towed-streamer acquisition. Consequently,

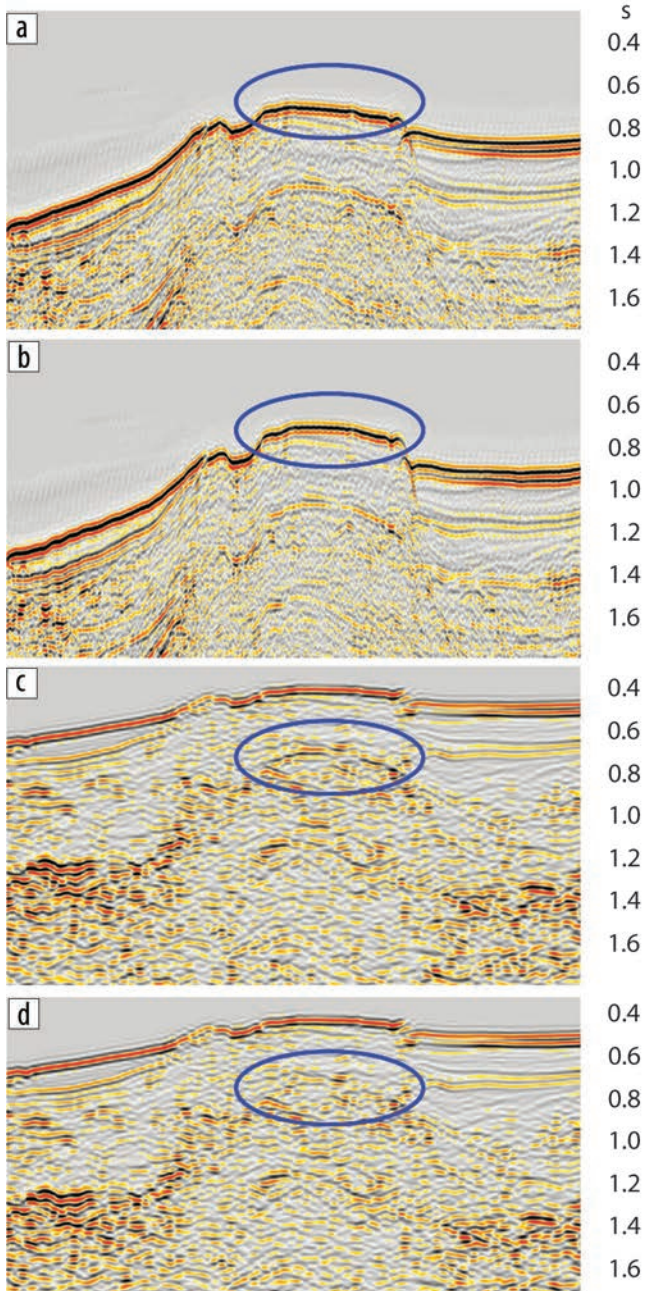

Figure 3. Near-channel model-based water-layer demultiple (MWD) results. Multiples predicted using a horizon interpreted from (a) standard RTM and (b) RTMM. Demultiple output using water-bottom horizon determined by (c) standard RTM and (d) RTMM. Courtesy of CGG. Used by permission.

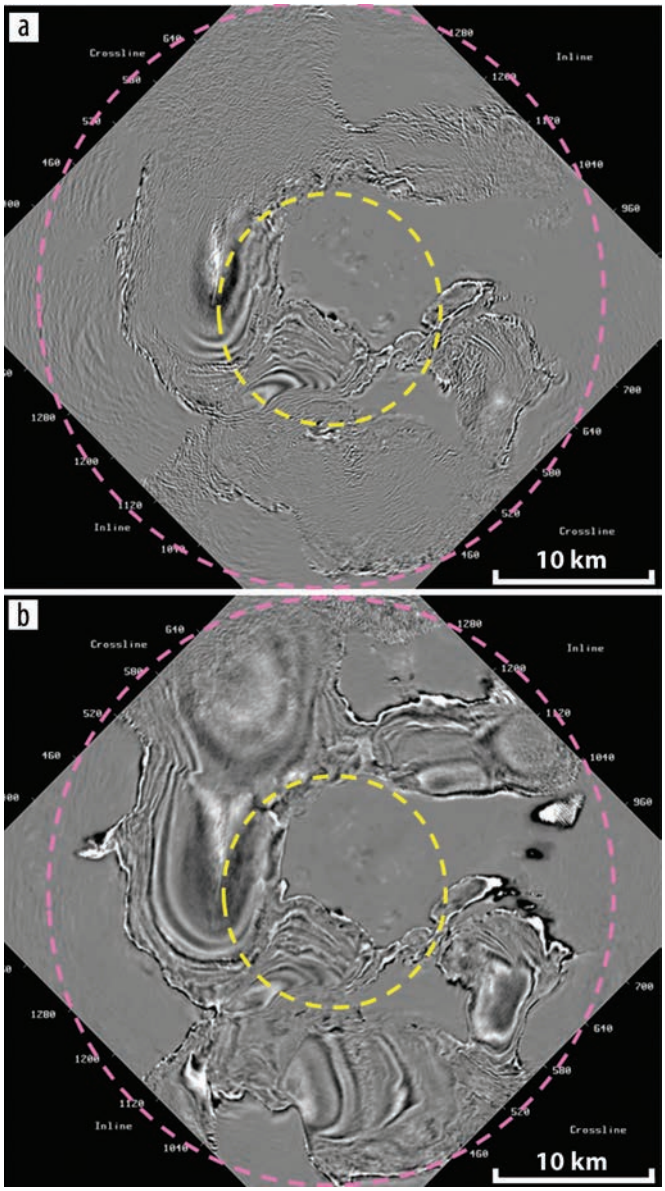

Figure 4. Depth-slice view at 2.9 km of (a) standard downgoing RTM image and (b) RTMM downgoing image. Courtesy of Chevron Corporation. Used by permission.

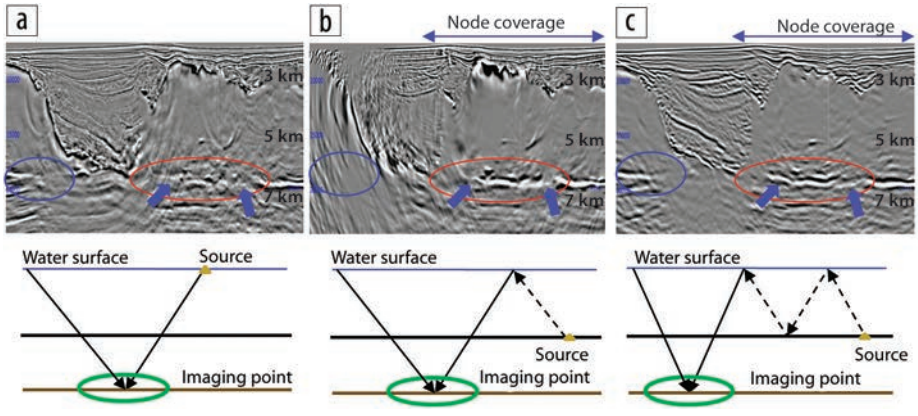

Figure 5. Salt-flood images at inline view: (a) WATS RTM, (b) OBN RTM, and (c) OBN RTMM. The corresponding raypath diagram is shown below each image. Courtesy of Chevron Corporation. Used by permission.

coverage of the nodes on the seafloor normally is limited, and it targets a particular subsurface structure. Shots from an OBN acquisition usually have a larger coverage and higher density on the sea surface. Ocean-bottom node imaging normally is performed in the common-receiver domain, in which each node is treated as a "supershot," and all surface shots contributing to this node are treated as receivers for this "supershot." Reverse time migration of multiples uses a pseudosurface source, which is the primary wavefield recorded at all receivers. That is, from the migration point of view, OBN standard RTM has low shot density and limited shot coverage (node density and coverage on the seafloor), but OBN RTMM has high shot density and larger shot coverage (shot density and coverage on the sea surface). Ocean-bottom node acquisition geometry is ideal to use the full potential of RTMM imaging.

Ocean-bottom node acquisitions record both the upgoing and downgoing wavefields. For simplicity, we will present only the comparisons of downgoing wavefield imaging, although a similar conclusion can be reached for upgoing wavefield imaging.

Figure 4 presents a comparison of the standard RTM image and the RTMM image in a depth-slice view at a depth of 2.9 km. Dashed pink and yellow circles indicate the shot and node coverage, respectively. The improvement of the RTMM image (Figure 4b) over the standard RTM image (Figure 4a) is significant.

The extra illumination not only helps to extend the image, but it also helps resolve complex salt geometry. We compared a salt-flood image in Figure 5. In several areas, the standard RTM using the OBN data (Figure 5b) already shows a better image at the base of salt (BOS) than the WATS data (Figure 5a). This indicates the benefit of the full-azimuth illumination provided by the OBN data, but the benefits are limited to the relatively small area covered by the nodes. By migrating the OBN data with RTMM, the illumination advantage is extended outside the nodes' coverage area for a better image of the BOS across the entire section (Figure 5c).

RTMM for WATS

The illumination benefit of RTMM on a WATS data set is not as obvious as the benefit for an OBN data set because WATS data typically extend far enough to provide all the apertures required for imaging. However, there are still areas of complex salt geometry where primary illumination is less than optimal, although multiple wavefields can provide a good complementary illumination. Figure 6 presents a real data example (WATS from the Gulf of Mexico) of RTMM that provides a complementary image to the primary image. The different illumination pattern of RTMM helps to image the subsalt events better (Figure 6b, red circle) compared with the standard RTM (Figure 6a, red circle).

Understanding cross-talk noise

Cross-talk noise undoubtedly is a major concern when one is applying RTMM. This cross-talk noise can be classified into two categories: (1) cross-order cross talk between different orders

of multiples and (2) cross-event cross talk formed by the complexity of the downgoing wavefield. To gain a better understanding of both types of cross talk, we conducted a 2D study on two synthetic models — the Sigsbee2b model and a flat reflector model.

For cross-order cross talk, we labeled the impulse wavefield from shot location as "order = 0," the primary wavefield as "order = 1," the first-order multiple as "order = 2," and so forth. Standard RTM applies an imaging condition between wavefields of order 0 and order 1, abbreviated as 0 * 1 (Figure 7a). The RTMM images used in the previous examples are 1 * 2 (Figure 7c). The majority of the cross-talk noise in RTMM was cross-order cross talk 1 * 3 + 4 (Figure 7d). In this unified picture, the multiple artifacts in the standard RTM also can be viewed as cross-order cross-talk noise 0 * 2 + 3 + 4 (Figure 7b). In fact, their raypath is nearly identical to 1 * 3 + 4, and the position of the noise in the stacked image matches well between standard RTM and RTMM (blue arrows). Thus, the natural strategy to handle this type of cross-talk noise is to separate different orders of multiples and apply imaging conditions only to the pairs that can form a correct image (the receiver side has one order higher than the source side).

The second type of cross-talk noise is cross-event cross talk, which can be more difficult to deal with than cross-order cross talk. To illustrate the challenges, we studied a simple synthetic model with multiple events imaging one flat reflector. The density model consisted of two closely spaced shallow flat reflectors and one deep flat reflector (Figure 8a). The velocity model was one constant value throughout. We attempted to use the reflected primary wavefield from the shallow reflectors to image the deep reflector with RTMM.

To simplify the demonstration further, we singled out the energy corresponding to the raypaths given in Figure 8a. Green raypaths were used for the primary wavefield (order 1), and blue raypaths were used for the first-order multiple wavefield (order 2). An interbed event between the two shallow reflectors was included unavoidably (far right of the raypath diagram). There was no cross-order cross talk here, and the image was formed solely by primaries and first-order multiple (1 * 2). However, once there were several events illuminating the same reflector, cross-event cross talk was generated.

Figure 8b shows several artificial layers in the RTMM image. To understand how the cross-event cross-talk noise was generated, snapshots of the source and receiver wavefields were captured and overlaid with the image. The red arrow points to the true location of the flat reflector to be imaged. If a downgoing source wavefront only "sees" its own reflected upgoing wavefront in the receiver wavefield, it will form a proper image without cross talk. However, the same source wavefront also "sees" many other receiver wavefronts generated by neighboring events, and vice versa. Those "mismatched" pairs of source wavefronts and receiver wavefronts are the root cause of the cross-event cross-talk problem.

In practice, vector-offset-output (VOO) (Xu et al., 2011) nonlinear stacking could be the most realistic and effective way to handle cross-event cross-talk noise in areas with sufficient 3D effect to enable us to separate events into different VOO sectors. The VOO sectors effectively decompose a stack image into separate dipping components. With the help of a guiding reference volume or reference dip field, the VOO sectors merge back into a final stack image by a coherency metric or by structure conformal filtering. Figure 8c shows that nonlinear stacking of VOO sectors effectively reduces the cross-talk noise of RTMM. In areas where the geology is mostly flat and/or with parallel dips, cross-event cross-talk noise

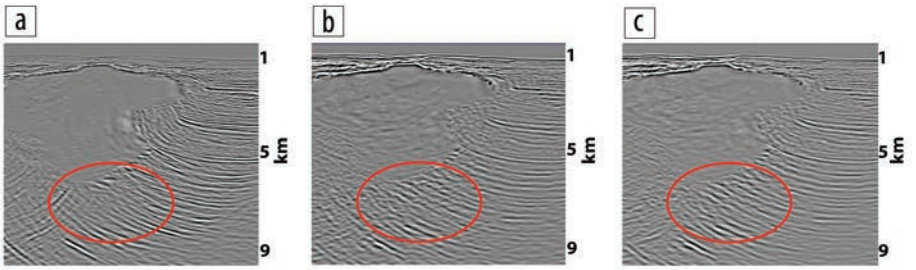

Figure 6. Wide-azimuth, towed-streamer (WATS) stack images from Gulf of Mexico: (a) standard RTM, (b) RTMM, and (c) RTMM with VOO sectors nonlinear stacking. Courtesy of CGG. Used by permission.

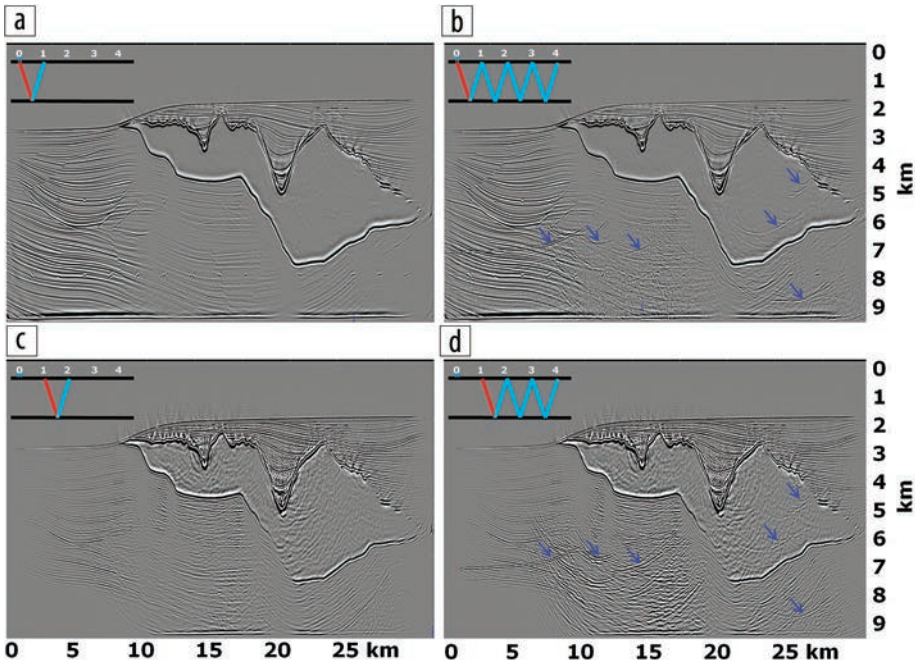

Figure 7. Study of cross-order cross-talk noise on the Sigsbee2b model. (a) Standard RTM 0 * 1 without multiple. (b) Standard RTM 0 * 1 + 2 + 3 + 4 with multiple. (c) RTMM 1 * 2 without higher-order multiple. (d) RTMM 1 * 2 + 3 + 4 with higher-order multiple. Courtesy of CGG. Used by permission.

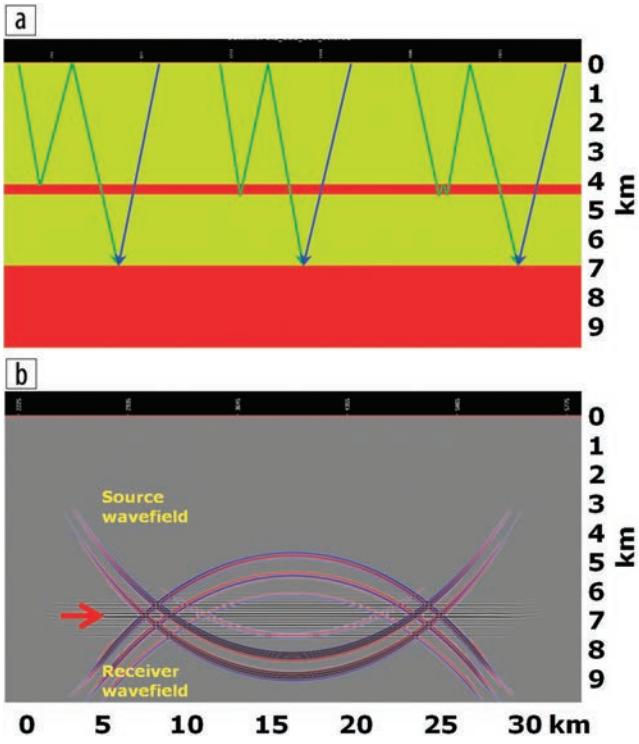

Figure 8. Study of cross-event cross-talk noise on a flat reflector model. (a) Density model overlaid with selected raypaths for source (green) and receiver (blue) wavefields. (b) RTMM image overlaid with source and receiver wavefields at a given time step. Courtesy of CGG. Used by permission.

could remain a significant challenge. Currently, there is no widely accepted solution to the cross-talk noise problem of multiple migration. Least-squares inversion is a good candidate, and there have been efforts in this direction with promising results using OBN data (Wong et al., 2014).

Conclusion

We presented three applications of RTMM using real data sets. For shallow-water demultiple, RTMM produces a better waterflood seismic image for the water-bottom event, leading to a more accurate water-bottom horizon, which thus helps to achieve a better result for MWD. For OBN acquisitions, RTMM significantly extends the imaging coverage and better defines the complex salt geometry. For WATS acquisitions, illumination of standard RTM might be less than optimal in certain places because of the geology, whereas RTMM can provide a complementary image to enhance the overall imaging of the subsurface structure.

The main challenge of RTMM is cross-talk noise. Cross-order cross talk can be handled by separating different orders of wavefields and applying imaging conditions only to the pair that can yield a correct image. Cross-event cross-talk noise is more difficult to address. The VOO nonlinear stacking is a practical and effective way to address both types of noise. TLE

Acknowledgments

We thank John Chen and Bassel Almoughraby from Chevron for permission to show these OBN real data examples. We thank Shuo Ji and Leon Chernis for their contribution in the development of RTMM. We thank SEG for the SEAM model and SMAART JV for the Sigsbee2b model. We thank CGG for permission to publish this work.

Corresponding author: ZhiPing.Yang@CGG.com

References

Berkhout, A. J., and D. J. Verschuur, 2011, Full wavefield migration, utilizing surface and internal multiple scattering: 81st Annual International Meeting, SEG, Expanded Abstracts, 3212–3216, http://dx.doi.org/10.1190/1.3627863.

Lu, S., N. D. Whitmore, A. A. Valenciano, and N. Chemingui, 2011, Imaging of primaries and multiples with 3D SEAM synthetic: 81st Annual International Meeting, SEG, Expanded Abstracts, 3217–3221, http://dx.doi.org/10.1190/1.3627864.

Wang, P., H. Jin, S. Xu, and Y. Zhang, 2011, Model-based water-layer demultiple: 81st Annual International Meeting, SEG, Expanded Abstracts, 3551–3555, http://dx.doi.org/10.1190/1.3627937.

Wong, M., B. Biondi, and S. Ronen, 2014, Imaging with multiples using least-squares reverse time migration: The Leading Edge, **33**, no. 9, 970–976, http://dx.doi.org/10.1190/tle33090970.1.

Xu, Q., Y. Li, X. Yu, and Y. Huang, 2011, Reverse time migration using vector offset output to improve subsalt imaging — A case study at the Walker Ridge GOM: 81st Annual International Meeting, SEG, Expanded Abstracts, 3269–3274, http://dx.doi.org/10.1190/1.3627875.

Yang, Z., L. Chernis, W. Gou, S. Ji, Y. Li, and J. Hembd, 2013, Enhanced reverse time multiple migration and its applications: 83rd Annual International Meeting, SEG, Expanded Abstracts, 4121–4125, http://dx.doi.org/10.1190/segam2013-0776.1.